ELSEVIER

Journal of Chromatography A, 776 (1997) 275–282

JOURNAL OF CHROMATOGRAPHY A

Chromatographic study of the influence of nitrogen dioxide on the reactions between volatile hydrocarbons and inorganic pigments

H. Zahariou-Rakanta, A. Kalantzopoulos, F. Roubani-Kalantzopoulou*

Department of Chemical Engineering, National Technical University of Athens, 15780 Zografou, Greece

Received 9 December 1996; revised 26 March 1997; accepted 3 April 1997

Abstract

Deposition velocities, V_d, reaction probabilities, γ, and local adsorption parameters, k_1, describing the isotherms of ethane, ethene, ethyne, propene and 1-butene onto three solid pigments (PbO, Fe_2O_3, CdS) have been determined in the absence and in the presence of NO_2, together with the surface reaction rate constant, k_2, and the desorption rate constant, k_{-1}. The calculations are based on experimental adsorption isotherms, since the linear adsorption model is not a very good approximation for inorganic solids like those mentioned above. The important result found is the effect of NO_2 on the values of the parameters V_d, γ, k_1, k_{-1} and k_2 in most cases. © 1997 Elsevier Science B.V.

Keywords: Adsorption isotherms; Kinetic studies; Reaction kinetics; Hydrocarbons; Nitrogen dioxide; Pigments

1. Introduction

Volatile hydrocarbons are emitted through a number of processes, the most important in urban areas being the combustion of organic fuels. Among the oxides of nitrogen that are present in polluted atmospheres, nitric oxide and nitrogen dioxide, designated by the composite formula NO_x, are the most important in relation to chemical and photochemical changes. Their major source is also fuel combustion.

The interaction of solid materials with the atmosphere has recently received increased attention as a result of concerns regarding the effects of acid deposition. In fact, most pollutants emitted into the atmosphere are eventually removed through capture by a sink or reservoir, where they are transformed, immobilized or encapsulated.

The reversed-flow gas chromatographic (RF-GC) method invented by Katsanos [1,2] is a powerful tool for the investigation and study of all corrosion phenomena through some simple chromatographic experiments. Lately, this method has been successfully applied to the study of the impact of air pollutants, organic and/or inorganic, on many solids such as marbles, stones, etc. [3–11]. The present work focuses on the determination of kinetic quantities for about thirty heterogeneous reactions including three known pigments, two oxides and one sulfide and five light hydrocarbons which exist in the atmosphere in great quantities, in the presence or not of the corrosive pollutant NO_2. All measurements were based on the real experimental adsorption isotherms, not necessarily linear [5], which are the

*Corresponding author.

0021-9673/97/$17.00
PII S0021-9673(97)00340-3

only correct ones for such studies. This type of isotherm is very rare in the literature.

2. Experimental

An outline of the experimental set-up is given in Fig. 1. The sampling cell, comprising the sampling column $l'+l$ (55 cm+55 cm×3.9 mm I.D.), the diffusion column L_1 (49 cm×3.9 mm I.D.) and the vessel L_2 (5.5 cm×24 mm I.D.), or L_1 (22 cm×3.5 mm I.D.) and L_2 (9.3 cm×3.5 mm I.D.) is accommodated inside the oven of a gas chromatograph equipped with a flame ionization detection (FID) system.

The solid pigment was placed inside vessel L_2 and heated in situ at 200°C for 24 h, under a continuous flow of carrier gas (99.99% nitrogen). Following this, the sampling cell was thermostated at the working temperature and an injection of 1–1.2 cm^3 gaseous mixture at atmospheric pressure was made, consisted of C_xH_y–NO_2 (20:1, v/v) or of pure C_xH_y.

The gaseous reactant injected and the possible gaseous products diffuse into the carrier gas, inside column L_1, creating finite gas concentrations at the junction $x=l'$ (cf. Fig. 1). On reversing the direction of the carrier gas flow every 2 min for 10 s, by means of the four-port valve, extra chromatographic peaks (sample peaks) appear superimposed on the continuous elution curve. These are predicted by the general chromatographic sampling equation ([1], p. 102) and their height H from the continuous signal or the area under the curve f, measure the concentration of gaseous analytes at the function $x=l'$ of Fig. 1, at time t. Examples of sample peaks are given in Fig. 2.

The external porosities and the specific surface areas of the three solids, required for the next calculations, were determined by the mercury-penetration method with a Porosimeter 2000 instrument, Milestone 200 and the nitrogen-desorption method with a Sorptomatic 1900 instrument, also Milestone 200. Table 1 lists the results of these measurements.

All gases were obtained from Air Liquide (Athens, Greece) and had a purity of better than 99%. The solids were analytical-reagent grade products (Merck).

3. Calculations

It is known [1,2,12] that the calculation of physicochemical parameters in the RF-GC method is based on a theoretical analysis of the diffusion band, obtained by plotting $H^{1/M}$ or $(1/M)$ ln H against t, where M is the response factor of the detector (1 for the linear, FID) and t the time when the respective flow reversal was made. The theoretical analysis depends each time on the phenomena being studied and the mathematical model employed. In most cases it leads to the sum (or difference) of four, three or

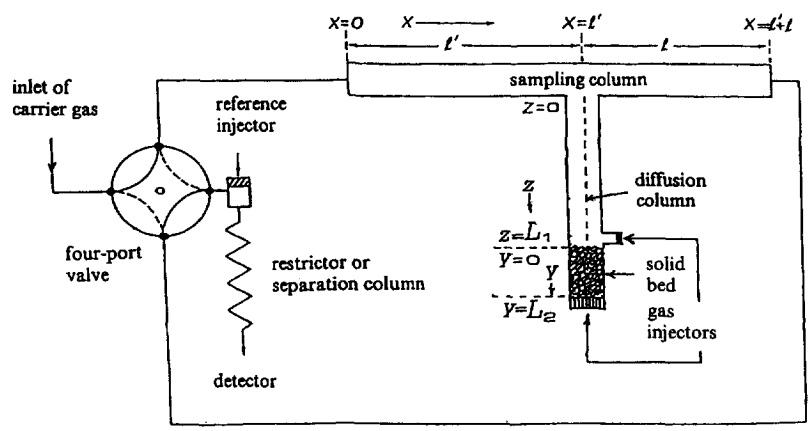

Fig. 1. Schematic representation of the columns and gas connections for the study of heterogeneous reactions between a pigment and one or two gases. From Ref. [10].

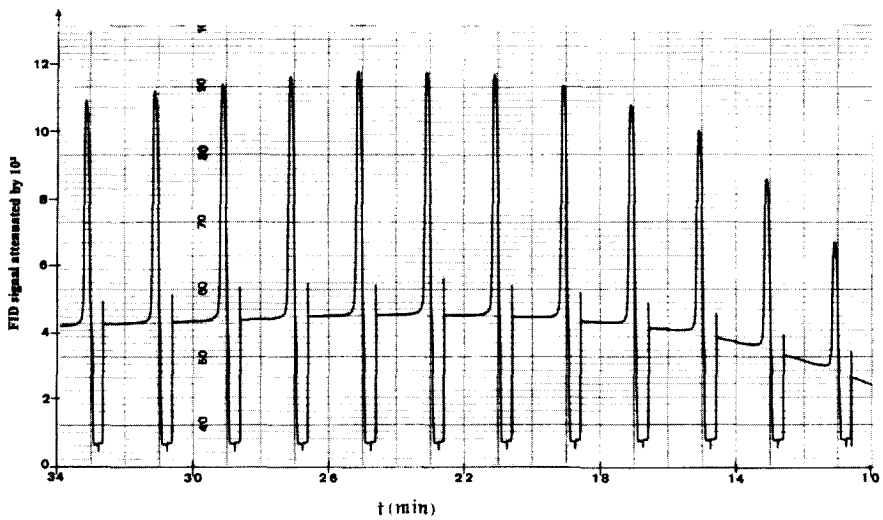

Fig. 2. Sample peaks of C_2H_6 and NO_2 in nitrogen in the presence of CdS at $T=323.2$ K.

two exponential functions of time, describing the diffusion bands, i.e.,

$$H^{1/M} = A_1\exp(B_1t) + A_2\exp(B_2t) + A_3\exp(B_3t) + A_4\exp(B_4t) \quad (1)$$

$$H^{1/M} = A_5\exp(B_5t) + A_6\exp(B_6t) + A_7\exp(B_7t) \quad (2)$$

The physical content of the pre-exponential factors A_1, A_2, A_3, A_4, A_5, A_6 and A_7 and the exponential coefficients of time B_1, B_2, B_3, B_4, B_5, B_6 and B_7, however, is different each time, depending on the mathematical model used, which in turn depends on the physicochemical quantities being sought. For the present purpose the calculations were based on a mathematical model of another paper [13], giving in detail the solution of a system of partial differential equations comprising: (1) The mass balance equation for the gaseous analyte being studied in the gaseous region z of the diffusion column (cf. Fig. 1); (2) the mass balance equation of A in region y, filled with the solid under study; (3) the rate of change of the concentration of the analyte A adsorbed on the solid surface; (4) the definition of the local adsorption isotherm, describing the relation between gaseous and adsorbed concentration of A in region y. This general definition of the isotherm equation suffices, so that the real experimental isotherm is automatically incorporated into the final calculations.

Table 1
External porosity ϵ and specific surface area SSA, measured for each pigment

Solid	ϵ	SSA ($m^2\,g^{-1}$)
PbO	0.5551	0.03
Fe_2O_3	0.7988	2.34
CdS	0.7425	2.51

The above system of differential equations was written in a precise mathematical form and solved analytically recently [13]. Here only the results applied to the present systems are quoted:

$$X = \alpha_2(1+V_1) + 2k_{app} + k_{-1} + k_2 = -(B_1 + B_2 + B_3 + B_4) \quad (3)$$

$$Y = [\alpha_2(1+V_1) + 2k_{app}](k_{-1} + k_2) + \alpha_1\alpha_2 + k_1k_{-1} + k_{app}^2 + \alpha_2(1+V_1)k_{app} = B_1B_2 + B_1B_3 + B_1B_4 + B_2B_3 + B_2B_4 + B_3B_4 \quad (4)$$

$$Z = \alpha_1\alpha_2(k_{-1} + k_2) + \alpha_2V_1k_1k_{-1} + k_1k_{-1}k_2 + \alpha_2(1+V_1)(k_{-1} + k_2)k_{app} + k_1k_{-1}k_{app} + k_{app}^2(k_{-1} + k_2) = -(B_1B_2B_3 + B_1B_2B_4 + B_1B_3B_4 + B_2B_3B_4) \quad (5)$$

$$W=(\alpha_2 V_1 + k_{app})k_1 k_{-1} k_2 = B_1 B_2 B_3 B_4 \quad (6)$$

where B_1, B_2, B_3 and B_4 are the exponential coefficients of time in Eq. (1), by means of which the auxiliary parameters X, Y, Z and W are calculated. The physicochemical parameters k_1, k_{-1}, k_2 and k_{app}, appearing in Eqs. (3)–(6) are defined [13] as k_1 = dynamic adsorption rate constant of the analyte pollutant A describing the local experimental isotherm on the surface of the solid, changing with time (s^{-1}); k_{-1} = desorption rate constant of A from the solid surface (s^{-1}); k_2 = rate constant of a possible first – or pseudo-first – order surface reaction of the adsorbed analyte A (s^{-1}); k_{app} = apparent first-order rate constant of a chemical reaction of A with another pollutant B in the gaseous phase above the solid, pertaining to synergistic effects (s^{-1}); D_1, D_2 = diffusion coefficients of A in the gas phase in regions z and y, respectively ($cm^2\ s^{-1}$).

The diffusion parameters α_1 and α_2 are defined by the relations

$$\alpha_1 = \frac{2D_1}{L_1^2}, \quad \alpha_2 = \frac{2D_2}{L_2^2} \quad (7)$$

and the dimensionless volume V_1 by

$$V_1 = \frac{2V'_G(\text{empty})\epsilon}{V_G} + \frac{\alpha_1}{\alpha_2} \quad (8)$$

L_1 and L_2 being the lengths of the sections z and y of the diffusion column, respectively, V_G and V'_G their gaseous volumes and ϵ the external porosity of the solid bed.

A steady-state assumption for the adsorbed concentration leads to Eq. (2). Instead of Eqs. (3)–(6) and the following relations are valid:

$$X_1 = \alpha_2(1+V_1) + 2k_{app} = -(B_5 + B_6 + B_7) \quad (9)$$

$$Y_1 = \alpha_1\alpha_2 + \frac{k_1 k_{-1} k_2}{k_{-1}+k_2} + \alpha_2(1+V_1)k_{app} + k_{app}^2 = B_5B_6 + B_5B_7 + B_6B_7 \quad (10)$$

$$Z_1 = \frac{(\alpha_2 V_1 + k_{app})k_1 k_{-1} k_2}{k_{-1}+k_2} = -(B_5B_6B_7) \quad (11)$$

Using the PC program of the appendix in Ref. [13], one can calculate the exponential coefficients of time B_1, B_2, B_3, B_4, B_5, B_6 and B_7 of Eqs. (1) and (2), and from them the auxiliary parameters X, Y, Z, W, X_1, Y_1 and Z_1. This calculation is based on a non-linear least square fitting to polyexponential functions of the experimental pairs of values H, t, where H is the height (in arbitrary units, say cm) of the sample chromatographic peaks and t the respective times, when flow-reversal of the carrier gas was made. This fitting is based on a FORTRAN IV computer program of Sedman and Wagner [15], dealing with polyexponential parameter estimates. As one can see from the appendix of Ref. [13], the program used is not a single seven exponential function for extracting B_1, B_2,..., B_7 from the experimental H, t values, but two functions, one with four exponential and the other with three exponential. The exponential stripping method [15] is guided by the overall goodness of fit expressed by the square of correlation coefficient r^2. This universally accepted criterion is calculated according to Eq. (5) of Ref. [15]. The maximum values of r^2 for the four and three exponential functions finally selected are printed, and here are given as r_4^2, r_3^2 in the last column of Tables 2–4. It is seen that the r^2 values fall in the range 0.9819–0.9998, showing a remarkable goodness of fit for a non-linear regression analysis. The t test of significance for the smallest r^2 found (0.9819), shows that it is highly significant, with a probability to be exceeded smaller than 0.05%. The program also prints, together with the B values, their standard errors and these are reasonable for physicochemical measurements in all runs.

From the auxiliary coefficients X, Y, Z, W, X_1, Y_1 and Z_1 by using Eqs. (3)–(11), the calculation of k_1, k_{-1}, k_2, k_{app} and a_1 is carried out.

The α_2 value is calculated in another experiment, using only A in the absence of a second pollutant B, when $k_{app}=0$ in all Eqs. (3)–(11). Finally, the overall deposition velocity V_d ($cm\ s^{-1}$) and the reaction probability γ of the analyte pollutant A on the solid material under study are found by the relations

$$V_d = \frac{k_1 V'_G(\text{empty})\epsilon}{A_s}\frac{k_2}{k_{-1}+k_2} \quad (12)$$

$$\frac{1}{\gamma} = \left(\frac{R_g T}{2\pi M_B}\right)^{1/2}\frac{1}{V_d} + \frac{1}{2} \quad (13)$$

where A_s = total surface area of solid (cm^2); R_g = ideal gas constant ($J\ K^{-1}\ mol^{-1}$); M_B = molar mass

Table 2
Local adsorption parameters (k_1), desorption rate constants (k_{-1}), surface reaction rate constants (k_2), deposition velocities (V_d), reaction probabilities (γ) and apparent gaseous reaction rate constants (k_{app}), of gaseous hydrocarbons C_xH_y (3.2×10^{-3} M), interacting with the PbO surface, in the absence and in the presence of gaseous NO_2 (1.6×10^{-4} M) at 323.2 K

Gaseous system	k_1 (10^{-4} s^{-1})	k_{-1} (10^{-4} s^{-1})	k_2 (10^{-4} s^{-1})	V_d (cm s^{-1})	γ	k_{app} (10^{-4} s^{-1})	r_4^2	r_3^2
C_2H_2[a]	5739	0.0322	28.9	2.45×10^{-4}	1.91×10^{-8}	–	0.9994	0.9994
C_2H_2–NO_2	12.8	50.8	5.06	4.95×10^{-8}	3.86×10^{-12}	7.43	0.9997	0.9996
C_2H_4	1246	0.488	3.72	4.71×10^{-5}	3.81×10^{-9}	–	0.9998	0.9998
C_2H_4–NO_2	1.22	23.4	15.0	2.03×10^{-8}	1.64×10^{-12}	6.93	0.9991	0.9989
C_2H_6[a]	10.0	64.5	15.9	8.45×10^{-8}	7.08×10^{-12}	–	0.9992	0.9991
C_2H_6–NO_2	27.8	32.2	1.83	6.39×10^{-8}	5.35×10^{-12}	43.2	0.9997	0.9993
C_3H_6[a]	6.37	35.2	14.9	8.10×10^{-8}	8.03×10^{-12}	–	0.9998	0.9995
C_3H_6–NO_2	0.0546	161	197	1.26×10^{-8}	1.25×10^{-12}	0.795	0.9968	0.9968
1-C_4H_8[a]	5.11	5.75	23.6	2.89×10^{-7}	3.31×10^{-11}	–	0.9984	0.9978
1-C_4H_8–NO_2	37.7	0.624	8.94	1.50×10^{-6}	1.72×10^{-10}	17.7	0.9983	0.9982

The goodness of curve fitting is given by the squared correlation coefficient for both, the four exponential and the three exponential functions (r_4^2, r_3^2).
[a] Obtained from Ref. [14].

of analyte A (kg mol^{-1}); T=absolute temperature (K).

All above calculations are effected by the same personal computer program mentioned above [13].

4. Results and discussion

In Fig. 3 an example of diffusion bands appears. It comprises four bands, one for the hydrocarbon alone, the second for the gaseous mixture of hydrocarbon–NO_2, the third for the heterogeneous system hydrocarbon–pigment and the fourth for the system hydrocarbon–NO_2–pigment.

All the calculated constants are listed in Tables 2–4. They refer to the heterogeneous reactions C_xH_y + pigment and $C_xH_y + NO_2$ + pigment. The number of significant figures given in the tables is based on the standard errors of Bs printed by the program, as mentioned before. It is difficult to

Table 3
Local adsorption parameters (k_1), desorption rate constants (k_{-1}), surface reaction rate constants (k_2), deposition velocities (V_d), reaction probabilities (γ), and apparent gaseous reaction rate constants (k_{app}), of gaseous hydrocarbons C_xH_y (3.2×10^{-3} M), interacting with the Fe_2O_3 surface, in the absence and in the presence of gaseous NO_2 (1.6×10^{-4} M) at 323.2 K

Gaseous system	k_1 (10^{-4} s^{-1})	k_{-1} (10^{-4} s^{-1})	k_2 (10^{-4} s^{-1})	V_d (cm s^{-1})	γ	k_{app} (10^{-4} s^{-1})	r_4^2	r_3^2
C_2H_2[a]	16.0	47.8	21.6	1.63×10^{-8}	1.27×10^{-12}	–	0.9998	0.9995
C_2H_2–NO_2	6.64	25.1	38.4	1.32×10^{-8}	1.03×10^{-12}	6.88	0.9997	0.9987
C_2H_4[a]	0.0182	397	444	5.61×10^{-10}	4.54×10^{-14}	–	0.9990	0.9990
C_2H_4–NO_2	6.27	9.31	22.3	3.53×10^{-8}	2.86×10^{-12}	0.977	0.9998	0.9998
C_2H_6[a]	13.4	11.3	20.3	2.83×10^{-8}	2.37×10^{-12}	–	0.9997	0.9997
C_2H_6–NO_2	94.7	4.05	40.8	3.45×10^{-7}	2.89×10^{-11}	8.15	0.9997	0.9997
C_3H_6[a]	0.0094	521	560	4.48×10^{-10}	4.44×10^{-14}	–	0.9996	0.9995
C_3H_6–NO_2	1.37	21.8	46.0	8.58×10^{-9}	8.50×10^{-13}	0.763	0.9992	0.9990
1-C_4H_8[a]	527	0.0821	0.338	2.28×10^{-6}	2.61×10^{-10}	–	0.9995	0.9993
1-C_4H_8–NO_2	166	0.382	0.720	1.17×10^{-6}	1.33×10^{-10}	0.943	0.9992	0.9991

The goodness of curve fitting is given by the squared correlation coefficient for both, the four exponential and the three exponential functions (r_4^2, r_3^2).
[a] Obtained from Ref. [14].

Table 4
Local adsorption parameters (k_1), desorption rate constants (k_{-1}), surface reaction rate constants (k_2), deposition velocities (V_d), reaction probabilities (γ), and apparent gaseous reaction rate constants (k_{app}), of gaseous hydrocarbons C_xH_y (3.2×10^{-3} M), interacting with the CdS surface, in the absence and in the presence of gaseous NO_2 (1.6×10^{-4} M) at 323.2 K

Gaseous system	k_1 (10^{-4} s^{-1})	k_{-1} (10^{-4} s^{-1})	k_2 (10^{-4} s^{-1})	V_d (cm s^{-1})	γ	k_{app} (10^{-4} s^{-1})	r_4^2	r_3^2
C_2H_2	10.1	23.6	0.275	3.55×10^{-10}	2.77×10^{-14}	–	0.9980	0.9974
C_2H_2–NO_2	4.89	75.4	0.580	1.14×10^{-10}	8.93×10^{-15}	2.75	0.9964	0.9949
C_2H_4	5.28	48.4	0.562	1.86×10^{-10}	1.50×10^{-14}	–	0.9974	0.9971
C_2H_4–NO_2	5.73	21.0	0.541	4.42×10^{-10}	3.57×10^{-14}	6.22	0.9929	0.9925
C_2H_6	6.92	70.6	0.476	1.42×10^{-10}	1.19×10^{-14}	–	0.9988	0.9973
C_2H_6–NO_2	5.61	55.8	0.614	1.87×10^{-10}	1.57×10^{-14}	3.08	0.9990	0.9819
C_3H_6	13.1	0.190	11.2	3.96×10^{-8}	3.93×10^{-12}	–	0.9967	0.9942
C_3H_6–NO_2	0.486	55.1	2.43	6.29×10^{-11}	6.23×10^{-15}	3.91	0.9976	0.9943
$1-C_4H_8$	4.04	35.1	0.265	9.27×10^{-11}	1.06×10^{-14}	–	0.9985	0.9946
1-C_4H_8–NO_2	3.05	33.1	0.136	3.84×10^{-11}	4.39×10^{-15}	1.69	0.9995	0.9945

The goodness of curve fitting is given by the squared correlation coefficient for both, the four exponential and the three exponential functions (r_4^2, r_3^2).

estimate the final errors of the parameters k_1, k_{-1}, k_2, V_d, γ and k_{app}, since they come out as a result of complex algebraic calculations based on Eqs. (3)–(13). The application of the law of propagation of errors in a long sequence of steps does not give reliable final errors. This was printed out before by Katsanos and Kapolos [16]. Thus, 55 physicochemical quantities have been calculated for each solid, 165 kinetic constants in total. It is obvious that from these systematic experiments, providing numerous results, one can be led to some conclusions about the influence itself and the mechanism of the alkanes, alkenes and alkynes on the three solids used, in the absence and in the presence of NO_2.

NO_2 is a powerful oxidizing reagent with various possible oxidizing effects. The catalytic effects of NO_2 on the reactions between the various hydrocarbons studied and some of the pigments used are demonstrated by the different values of the experimentally obtained deposition velocities and re-

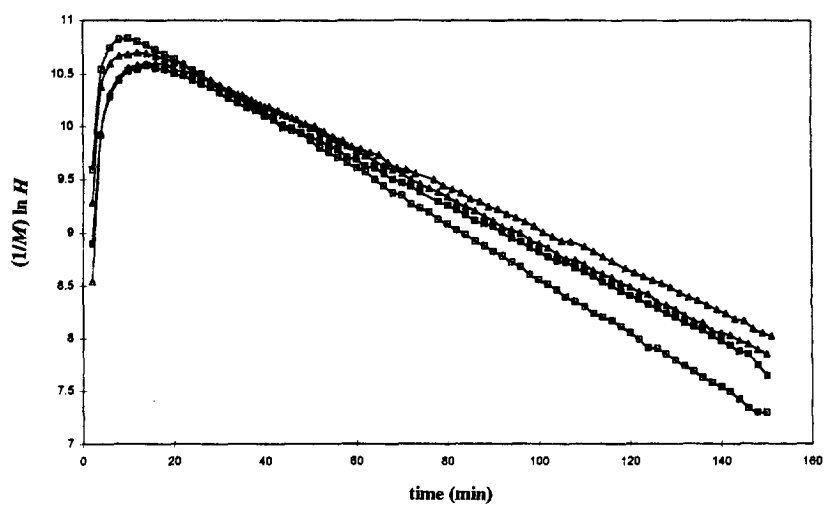

Fig. 3. Diffusion bands obtained for the following four systems, (□) C_2H_4, (■) C_2H_4–NO_2, (△) C_2H_4–PbO, (▲) C_2H_4–NO_2–PbO, with a volume ratio C_2H_4–NO_2 = 20:1.

action probabilities in most cases. Among the various kinds of the hydrocarbons studied with the RF-GC technique, some of them appear more reactive than the others. Obviously, to explain the influence of NO_2 on the various physicochemical parameters, one needs some knowledge about the detailed mechanism of the phenomena, which almost certainly include blocking of adsorption active sites by NO_2 molecules or creation of new ones by it. The kinetic model that describes these gas–solid interactions may be the following: (cf. Fig. 4).

When the pollutants reach the pigment surface, an adsorption process is possible leading to the adsorbed species and followed by the final products of the heterogeneous reactions. The product of the possible homogeneous reaction may have the same behaviour. All these interactions may be reversible. Bimolecular reactions between the adsorbed compounds are also possible, but it is very difficult to be described quantitatively. This is the reason that they have not been included in Fig. 4.

What, in reality, will have a major significance in the future is the identification of all these intermediates and final products mentioned, by the appropriate techniques. But the present work enables us to investigate whether a synergy exists between these pollutants and solids and that is achieved through the calculation of the six fundamental physicochemical quantities pertaining to any of the thirty heterogeneous reactions. These values constitute a wealth of information showing what a simple gas chromatographic arrangement can offer to surface and atmospheric chemists and chemical engineers, instead of the conventional global rate constants.

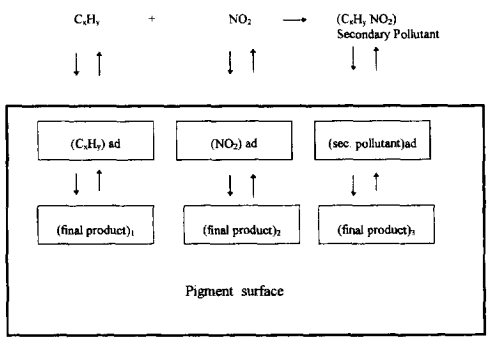

Fig. 4. Possible homogeneous and heterogeneous interactions among pollutants and pigment surface.

Hence the most important result is that the experimentally observed values of deposition velocity, V_d, and reaction probability γ are influenced by the presence of NO_2 in most cases. Probably, the synergistic effects between hydrocarbons and NO_2 lead to much greater damage and corrosion of these pigments in some cases, and perhaps of many others. As these pigments have been widely used as paints for many works of art, the significance of these results is obvious. Thus the coexistence of light hydrocarbons with NO_2 on the pigments' surface has a great economic and social impact.

5. Conclusions

The RF-GC technique was used to study the kinetics of thirty heterogeneous reactions from which the significant role of NO_2 existence is concluded. A combination of the mathematical analysis developed in homogeneous and heterogeneous catalysis, mass transfer across gas–solid interfaces and diffusion of gases was employed to find the final equations. It has become obvious from the results that all these physicochemical parameters obtained are not easily accessible by other conventional techniques. It remains to apply this method under conditions of a sunlight-irradiated atmosphere for the determination of the photochemical processes apart from the physical and chemical ones and the study of more complex and more realistic systems and interactions.

Acknowledgments

The authors acknowledge the financial support from the European Commission with the contract EV5V-CT94-0537.

References

[1] N.A. Katsanos, Flow Pertubation Gas Chromatography, Marcel Dekker, New York, Basel, 1988, pp. 87–111.
[2] N.A. Katsanos, in F. Dondi and G. Guiochon (Editors), Theoretical Advancement in Chromatography and Related Separation Techniques, Kluwer Academic Publishers, Dordrechht, 1992, pp. 339–367.

[3] E. Arvanitopoulou, N.A. Katsanos, H. Metaxa, F. Roubani-Kalantzopoulou, Atmos. Environ. 28 (1994) 2407.
[4] E. Arvanitopoulou, V. Sotiropoulou, N.A. Katsanos, H. Metaxa and F. Roubani-Kalantzopoulou, in V. Fassina, H. Ott and F. Zezza (Editors), Proceedings of the 3rd International Symposium of the Conservation of Monuments in the Mediterranean Basin, Venice, 1994, p. 195.
[5] V. Sotiropoulou, G.P. Vassilev, N.A. Katsanos, H. Metaxa, F. Roubani- Kalantzopoulou, J. Chem. Soc. Faraday Trans. 91 (1995) 485.
[6] N.A. Katsanos, F. Roubani-Kalantzopoulou, J. Chromatogr. A 710 (1995) 191.
[7] N.A. Katsanos, V. Sotiropoulou, F. Roubani-Kalantzopoulou and H. Metaxa, International Conference on Ozone in the Lower Stratosphere, Halkidiki, Greece, 1995, p. 254.
[8] N.A. Katsanos, V. Sotiropoulou, F. Roubani-Kalantzopoulou and H. Metaxa, 8th National Meeting on Chromatography, Sofia, Bulgaria, 1995; Anal. Lab. 5 (1996) 13.
[9] A. Kalantzopoulos, F. Roubani-Kalantzopoulou, J. Kapolos and N.A. Katsanos, Proc. 4th Panhellenic Symposium on Catalysis, Papigo, Greece 1995, p. 45.
[10] N.A. Katsanos, V. Sotiropoulou, F. Roubani-Kalantzopoulou and A. Kalantzopoulos, Proc. Intern. Congress on Environment/Climate ICEC-96, Rome, Italy, 1996, In press.
[11] F. Roubani-Kalantzopoulou, H. Metaxa, A. Kalantzopoulos and N.A. Katsanos, in R. Pancella (Editor), Preservation and Restoration of Cultural Heritage, Congress LPC 95, Montreux, Switzerland, 1995, p. 393.
[12] V. Sotiropoulou, N.A. Katsanos, H. Metaxa, F. Roubani-Kalantzopoulou, Chromatographia 42 (1996) 441.
[13] Ch. Abatzoglou, E. Iliopoulou, N.A. Katsanos, F. Roubani-Kalantzopoulou, A. Kalantzopoulos, J. Chromatogr. A 775 (1997) 211.
[14] F. Roubani-Kalantzopoulou, A. Kalantzopoulos and N.A. Katsanos, in preparation.
[15] A.J. Sedman, J.G. Wagner, J. Pharm. Sci. 65 (1976) 1006.
[16] N.A. Katsanos, J. Kapolos, Anal. Chem. 61 (1989) 2231.